Astronomical and Astrophysical Transactions (*AApTr*), 2016, Vol. 29, Issue 4, pp. 511–518,
ISSN 1055-6796, Photocopying permitted by license only, ©Cambridge Scientific Publishers

The indirect techniques of imaging and research of space object structures, including Doppler tomography

M.I. Agafonov*, E.N. Vinyajkin

Radiophysical Research Institute, Lobachevsky State University of Nizhni Novgorod

Received 15 September, 2015

The indirect techniques of imaging and research of space object structures are of considerable interest since they get information not available for present day telescopes. The tomographic methods are divided into two major classes. The main feature of the first one is using the rotation of the object under research. The second class does not relate to the object rotation. The Doppler tomography method in its three-dimensional form belonging to the first class is very informative. It is the most adequate to study gas flows in close binary star systems without assuming the existence of such flows only in the orbital plane. A short description of other tomographic methods is also presented.

Keywords: Astrotomography, Doppler tomography, binaries, algols, gas flows

1 Introduction

In spite of impressive achievements in astronomical object imaging by VLBIs, optical interferometers and orbital telescopes (Kardashev et al. 2013; Akiyama et al. 2015; Blind et al. 2011; Weisskopf et al. 2002) there is still a need for more high angular resolution. It is especially necessary in observations of close binaries, extragalactic sources or in observations of the more detailed structure of already partially resolved objects. As an example, the linear separation between centers of the components of the polar EXO033319-2554.2 with orbital period of 126.5 min (Cropper 1990) equals 0.86 $R_\odot$ that corresponds to the angular separation of 16 micro-arcseconds at a distance of 250 pc. Modern telescopes cannot provide such angular resolution that permits us to observe separately the components of this and similar polars. That is why numerous indirect methods commonly referred to as astrotomography (Cameron et al. 2004) have been created and are being developed to obtain information about spatial and velocity structure of a variety of astronomical systems. A classical example of indirect method application is a discovery of a "core-jet" radio structure

*Email: agfn@nirfi.unn.ru

of quasar 3C 273 by lunar eclipse method with an unreachable at the time in radio astronomy angular resolution (Hazard et al. 1963).

2 Astrotomographic methods and their classification

Astrotomography methods, in spite of their variety, can be conditionally divided into two large groups with respect to the astronomical object under research.

Some astrotomographic methods use the rotation of the astronomical object under research to obtain information about its structure: eclipse mapping (Cameron et al. 2004; Baptista 2004), Stokes imaging (Potter et al. 1998, 2004), Doppler tomography (Agafonov et al. 2009; Richards et al. 2012) and Roche tomography (Cameron et al. 2004; Watson, Dhillon 2004).

Table 1. Methods that use the rotation of an astronomical object.

Method	Physical event on which the method is based	Astronomical objects under study	Input data (what is observed)	Final result (data processing result)
Eclipse mapping (Cameron et al. 2004; Baptista 2004)	An eclipse of a rotating white dwarf accretion disk by a red-dwarf companion	Cataclysmic Variables (CVs)	Optical or IR eclipse light curves of an accretion disk	The structure, spectrum and time evolution of an accretion disc
Stokes imaging (Potter et al. 1998, 2004)	Linearly and circularly polarized cyclotron emission	White dwarf accreting matter and magnetic field in polars	Four Stokes parameter light curves as a function of orbital phase	2D image of white dwarf cyclotron emission areas in magnetic latitude and longitude coordinates
Doppler tomography (Agafonov et al. 2009; Richards et al. 2012)	Non-relativistic Doppler shift in spectral lines	Gas flows in close binary star systems of different types	Spectral line profiles covering one or more full orbital cycles	Image in the 3D velocity vector components space
Roche tomography (Cameron et al. 2004; Watson, Dhillon, 2004)	Secondary star line emission at different orbital phases	A Roche lobe-filling secondary star in CVs	Spectral line profiles and intensities at different orbital phases	Line intensity distribution on the surface of the Roche-lobe-filling star in CVs
Qualitative Solar Rotational Tomography (QSRT) (Morgan et al. 2009)	Scattering of photosphere light by corona free electrons	The solar corona	2D coronagraph images at different phases of solar rotation	The 3D distribution of the electron density in the solar corona in relative values

Table 1 summarizes the information on the main tomographic methods that use the rotation of the astronomical object under study to change the angle of observation.

Rotation periods of astronomical objects in many cases are too large and it is impossible to change an angle of observation due to the object rotation. So, other methods do not relate to the object rotation. Among these methods, for example, we can name the echo (or reverberation) mapping of active galactic nuclei (Bochkarev, Antokhin 1982; Antokhin, Bochkarev 1983; Blandford, McKee 1982; Peterson, Horne 2004), the gravitational lensing (microlensing) technique (Kuijken 2003; Hoekstra 2013; Cropper et al. 2013), the interstellar scintillation method (Wolszczan, Cordes 1987; Smirnova et al. 1996, 2014), and the Faraday tomography method (Brentjens, de Bruyn 2005; Macquart et al. 2012). A characteristic feature of these methods is the presence of an auxiliary intermediate body or a propagation medium of electromagnetic waves, which are actually a part of a ground-space telescope. Table 2 summarizes the information on the main tomographic methods that do not use the rotation of astronomical objects.

Table 2. Methods that do not use the rotation of an astronomical object.

Method	Physical event on which the method is based	Astronomical objects under study	Input data (What is observed)	Final result (data processing result)
Echo-mapping (Bochkarev, Antokhin 1982; Antokhin, Bochkarev 1983; Blandford, McKee 1982; Peterson, Horne 2004)	Reemission of variable ionizing continuum radiation of a central source in spectral lines by a broad line regions (BLR) clouds	Quasars, Seyfert I galaxies	Continuum ionizing radiation of a central source and delayed emission from an ambient BLR in lines from far UV to near IR	Diagrams in continuum intensity–line intensity, lag–ray velocity coordinates. Kinematics and structure of BLR, central black hole mass
Gravitational lensing (microlensing) technique (Kuijken 2003; Hoekstra 2013; Cropper et al. 2013)	Gravitational lensing	Extragalactic objects, stars, exoplanets	Lensed image of an astronomical object	Distribution of gravitating matter over lens and/or its mass
Interstellar scintillation method (Wolszczan, Cordes 1987; Smirnova et al. 1996, 2014)	Radio wave propagation effects in a randomly non-uniform interstellar medium	Pulsars, compact extragalactic radio sources	Scintillations of the radio emission intensity	Estimation of the radio source angular size. Spatial structure of pulsar radio emission sources

Table 2 (Continued)

Faraday rotation measure synthesis (Brentjens, de Bruyn 2005; Macquart et al. 2012)	The Faraday effect in a magnetized ionized interstellar medium	Galactic and extragalactic radio sources of synchrotron radiation	Wavelength squared dependence of the Stokes parameters over the radio source	Angular distribution of the intensity of the linear polarized radio emission component for different values of the Faraday depth
The method of lunar occultations (Hazard et al. 1963)	Diffraction of electromagnetic waves by the lunar limb	Galactic and extragalactic radio sources, stars	Occultation curves of a source transition for different values of the position angle	The angular distribution of the emission intensity over the source
Helioseismology and asteroseismology (Scherrer et al. 1995; Kosovichev et al. 2009)	Doppler shift caused by acoustic oscillations inside the Sun or a star	The Sun and a star interiors	Doppler shift oscillations of spectral lines in the visible light	Space distribution of the sound speed, chemical elements, the angular speed of rotation (and so on) inside the Sun and stars

The classification of tomography methods presented in Tables 1 and 2 which use or do not use the rotation of a space object is true in most cases, although there are examples of combinations of both approaches. For example, the rotation has been used in the gravitational microlensing method applied to a self-lensing binary star system (Kruse, Agol 2014). The method based on the object passive sensing at various wavelengths does not relate to the object rotation. This method should also be attributed to tomographic approaches since it gets information on the internal physical structure of the object layers located at different depths from its surface.

One way or another all astrotomography methods solve the inverse problem. Light curves, spectrograms, polarization characteristics, echo-signals, and so on are used to restore the radiation source structure, its kinematics and physical parameters. On the other hand, if the source properties are known, we can get information on the auxiliary object or the medium.

3 The 3D Doppler tomography

The method of Doppler Tomography (DT) (Marsh, Horne 1988) is used successfully in the study of binaries such as cataclysmic variables (CVs), algols, polars or X-ray binaries. The observational basis is one-dimensional profiles of the emission lines. If ephemerides are available, they are transformed into orbital phase values $\Phi(t)$, and the profiles are translated into radial velocity curves $V_R(\Phi)$. The Doppler tomogram reconstruction is performed on the basis of a set of profiles, which have been obtained with a high spectral resolution for one or several full orbital cycles. The tomogram corresponds to the distribution of the radiation intensity $I(V_x, V_y)$ at frequencies of some emission line in the velocity space. The 3D Doppler Tomography uses 3D velocity space (V_x, V_y, V_z).

The tomogram summarizes the emission of many detached components into the general picture and can show characteristic features of the matter flow. Under some assumptions, it makes possible to obtain the solution of the second problem – the transformation of the emission intensity distribution from the velocity space into the geometry space $I(V_x, V_y, V_z) \rightarrow I(x, y, z)$. The synthetic Doppler tomograms reconstructed from the results of the 3D gas-dynamic calculations have been presented in (Kuznetsov et al. 2001; Kononov et al. 2014). The comparison of such tomograms with those based on the observational data provides the best examination of the correctness of the characteristic feature recognition of the gas flow structure.

Although the general principle of DT (Marsh, Horne 1988) allows for the introduction of the third coordinate V_z, only a two-dimensional (standard) version of the method has been extended so far (see, for example, Steeghs 2004; Richards et al. 1995; Morales-Rueda 2004; Vrtilek et al. 2004; Richards 2004; Marsh 2005) where the result of the reconstruction corresponds to the intensity distribution map on the plane $I(V_x, V_y)$. It is clear, that the assumption introduced in the 2D Doppler tomography on the absence of gas flows in the directions different from the orbital plane of systems does not correspond to the physical nature of a number of objects.

Therefore, the realization and the development of the 3D DT with all three velocity components (V_x, V_y, V_z) is an urgent task for the new, more adequate information on the gas movements in interacting stellar systems. It was noted at the Discussion Session on Astrotomography at IAU General Assembly in 2003, as well as in (Steeghs 2004), to the prospect of the use of the 3D version $I(V_x, V_y, V_z)$ in order to obtain a more adequate physical picture, since a 3D-tomogram allows the display of movement of matter in all directions, not just in the orbital plane of the binary systems. The developed 3D version of the Radioastronomical Approach (RA) 3D1D (Agafonov, Sharova 2005 a, b) turned out to be very useful in the implementation of 3D tomography. The RA to the reconstruction is a method developed to solve problems of small-angle tomography (Agafonov 2004 a, b). In the 3D version, a rotating object is observed at different phase angles. However, it has a single (fixed) inclination angle. Hence, the 3D tomogram reconstruction relates to the problems of small-angle tomography. The summarized transfer function used by solution of this 3D deconvolution problem looks weakly filled in the spatial-frequency domain (Agafonov, Sidorov 2014). The RA reconstructs a 3D tomogram numeric array directly by 1D profiles without building 2D cross-sections at the intermediate stage. The 2D cross-sections can be obtained later at the stage of visualization of the numeric array

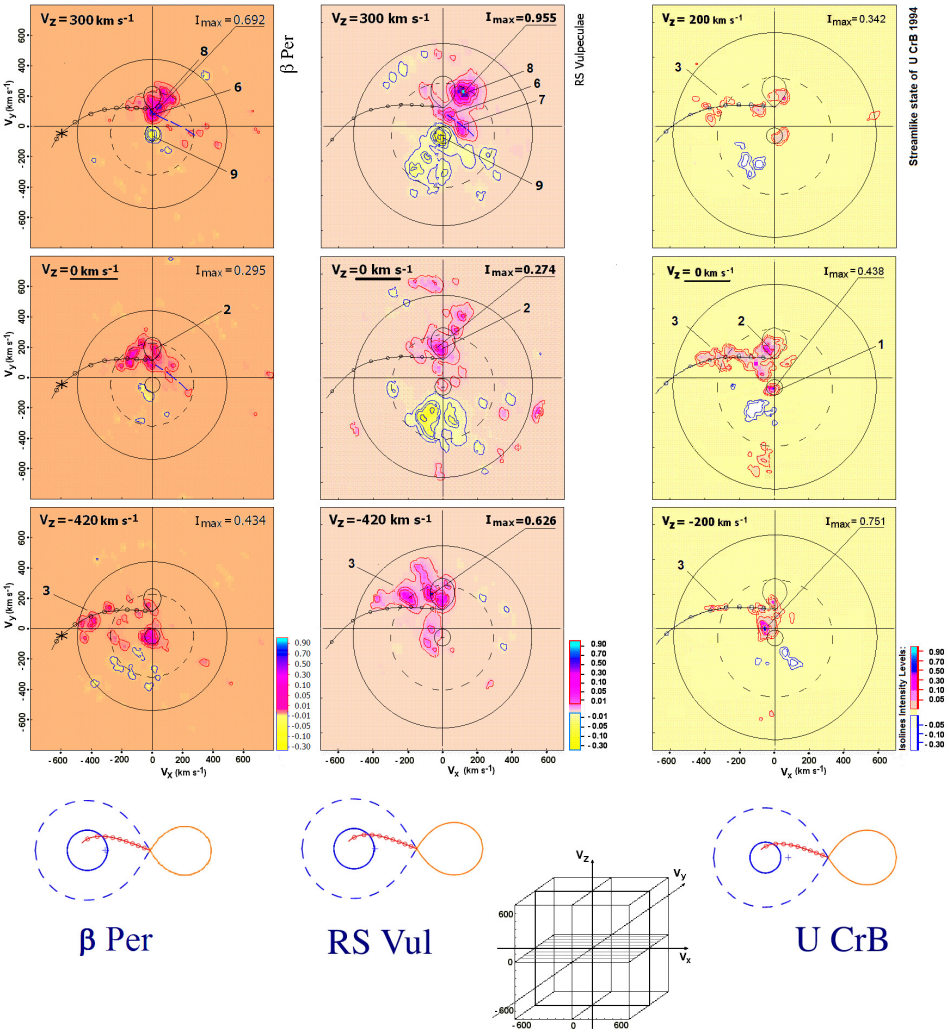


Figure 1 Visualization of the (V_x, V_y) slices in the 3D Doppler Tomograms of beta Per (Algol), RS Vul, U CrB in H-alpha line displayed for three values of V_z. The direction of V_z-axis is perpendicular to the orbital plane. The cube shows the position of the slices. The emission features are shown by the numbers: 1 – Circumprimary emission (accretor); 2 – Emission on donor star; 3 – Gas stream flow (from donor star to accretor); 6–7 – Localized region (superhump); 8 – High velocity flow near donor; 9 – Absorption zone. The Cartesian models of the three systems are shown in the lower part of the figure.

of the built 3D-tomogram. Figure 1 shows the sections of 3D Doppler tomograms of three Algol-type binaries (Agafonov et al. 2006, 2009; Richards et al. 2010, 2012), which has been realized for the first time in the world.

There are only three basic sections for each binary in Fig. 1; however, we see the fundamental differences in the behavior of the gas flows in these binaries. There

is an absence of an accretion disk for U CrB according to the observations in 1994 (Richards et al. 1995), and the gas flows to the accretor along the expected ballistic trajectory in the orbital plane (V_x, V_y) by $V_z = 0$ km s^{-1}. The inclination of the gas flows to the orbital plane has been discovered for both other binaries RS Vul and beta Per (Algol). This may be explained by the presence of the donor-star magnetic field. The possibility of magnetic interaction between the stars in Algol-type binaries has recently been confirmed for the beta Per by VLBI observations at 15 GHz (Peterson et al. 2010).

As a result, it has been found experimentally the presence of coronal mass ejections associated with the donor star and the declination of gas flows from the orbital plane in algols beta Per and RS Vul. The obtained results confirm the model of the magnetic activity in Algol-type binaries according to which there is an emission structure in the area between the stars as a result of the magnetic interaction between the accretion flow and dragged donor star magnetic field lines (Richards et al. 2012).

Conclusions

We have examined briefly all of the basic indirect mapping methods of astrotomography. They are classified into two classes and their properties are presented in Tables 1 and 2. The first class of the methods relates to the rotation of the sources and is a classical one in the sense of computerized reconstruction tomography. The methods of the second class are not based on the rotation of the sources and in this sense they are not so classical.

Each method requires significant adaptation of reconstruction algorithms for a specific problem. The Doppler tomography method is the more attractive one among the four others of the first class of methods. It gives very interesting information about the physical conditions in the sources. Its application allows us to study gas flows in the interacting binary star systems. The physical basis of the method is the non-relativistic Doppler shift in the spectra lines. The final result after the tomography reconstruction is a 2D image in the velocity space as a standard version or 3D image in cube for a 3D version. The spectra of emission lines obtained in wide optic-, UF- or IR ranges from ground or space observatories may be applied as the initial data.

Acknowledgements

We thank the Russian Foundation of Basic Research (RFBR) for partial support of the work (grants 15-02-02145 and 15-52-12371).

References

Agafonov M.I. (2004a) Radiophysics and Quantum Electronics 47, 85.
Agafonov M.I. (2004b) Astron. Nachrichten 325, 263.
Agafonov M.I., Sharova, O.I. (2005a) Radiophysics and Quantum Electronics 48, 329.

Agafonov M.I., Sharova O.I. (2005b) Astron. Nachrichten 326, 143.
Agafonov M.I., Richards M.T., Sharova, O.I. (2006) ApJ 652, 1547.
Agafonov M.I., Sharova O.I., and Richards, M.T. (2009) ApJ 690, 1730.
Agafonov M.I., Sidorov M.Yu. (2014) ARep 58, 481.
Akiyama K., Ru-Sen Lu, Fish V. L. et al. (2015) ApJ 807, 150.
Antokhin I.I., Bochkarev N.G. (1983) SvA 27, 261.
Baptista R. (2004) Astron. Nachrichten 325, 181.
Blandford R.D., McKee C.F. (1982) ApJ 255, 419.
Blind N., Boffin H.M.J., Berger J.-P. et al. (2011) A&A 536, A55.
Bochkarev N.G., Antokhin I.I. (1982) ATsir no.1238.
Brentjens M.A., de Bruyn A. G. (2005) A&A 441, 1217.
Cameron A.C., Schwope A., Vrielman S. (2004) Astron. Nachrichten 325, 179.
Cropper M. (1990) Space Science Reviews 54, 195.
Cropper M., Hoekstra H., Kitching T. et al. (2013) MNRAS 431, 3103.
Hazard C., Mackey M.B., Shimmins A.J. (1963) Nature 197, 1037.
Hoekstra H. (2013) arXiv:1312.5981v1 (astro-ph.CO).
Kardashev N.S., Khartov V.V., Abramov V.V. et al. (2013) ARep, 57, 153.
Kononov D.A., Agafonov M.I., Sharova O.I. et al. (2014) ARep 58, 881.
Kosovichev A., Zhao J., Sekii T. et al. (2009) ASP Conference Series, 415, 399.
Kruse E., Agol E. (2014) Science 344, 275; arXiv:1404.4379v1 (astro-ph.SR).
Kuijken K. (2003) arXiv: astro-ph/0304438v1.
Kuznetsov O.A., Bisikalo D.V., Boyarchuk A.A. et al. (2001) ARep 45, 872.
Macquart J.P., Ekers R.D., Feain I., Johnston-Hollitt M. (2012) ApJ 750: article id.139.
Marsh T.R., Horne K. (1988) MNRAS 235, 269.
Marsh T.R. (2005) Ap&SS 296, 403.
Morales-Rueda, L. (2004) Astron. Nachrichten 325, 193.
Morgan H., Habbal S. R., Lugaz, N. (2009) ApJ 690, 1119.
Peterson B.M., Horne K. (2004) Astron. Nachrichten 325, 248.
Peterson W.M., Mutel R.L., Gudel M., (2010) Nature 463, 207.
Potter S.B., Hakala P. J., Cropper M. (1998) MNRAS 297, 1261.
Potter S., Romero-Colmenero E., Buckley D.A.H. (2004) Astron. Nachrichten 325, 201.
Richards M.T., Albright G.E., Bowles L.M. (1995) ApJ 438, L103.
Richards M.T. (2004) Astron. Nachrichten 325, 229.
Richards M.T., Sharova O.I., Agafonov M.I. (2010) ApJ 720, 996.
Richards M.T., Agafonov M.I., Sharova O.I. (2012) ApJ 760: 8.
Scherrer P.H., Bogart R.S., Bush R.I. et al. (1995) Solar Physics 162, 129.
Smirnova T.V., Shishov V.I., Malofeev V.M. (1996) ApJ 462, 289.
Smirnova T.V., Shishov V.I., Popov M.V. et al. (2014) ApJ, 786: article id.115.
Steeghs D. (2004) Astron. Nachrichten 325, 185.
Vrtilek S.D., Quaintrell H., Boroson B., Shields M. (2004) Astron. Nachrichten 325, 209.
Watson C.A., Dhillon V.S. (2004) Astron. Nachrichten 325, 189.
Weisskopf M.C., Brinkman B., Canizares C. et al. (2002) 114, 1.
Wolszczan A., Cordes J. M. (1987) ApJ 320, L35.